

Low velocity impact behavior of concrete beam strengthened with CFRP strip

Erkan Kantar¹ and Özgür Anil*²

¹*Civil Eng. Dept., Celal Bayar University, Manisa, Türkiye, 45040*

²*Civil Eng. Dept., Gazi University, Maltepe, Ankara, Türkiye, 06570*

(Received October 14, 2010, Revised November 16, 2011, Accepted December 01, 2011)

Abstract. Nowadays CFRP (Carbon Fiber Reinforced Polymer) became widely used materials for the strengthening and retrofitting of structures. Many experimental and analytical studies are encountered at literature about strengthening beams by using this kind of materials against static loads and cyclic loads such as earthquake or wind loading for investigating their behavior. But authors did not found any study about strengthening of RC beams by using CFRP against low velocity impact and investigating their behavior. For these reasons an experimental study is conducted on totally ten strengthened RC beams. Impact loading is applied on to specimens by using an impact loading system that is designed by authors. Investigated parameters were concrete compression strength and drop height. Two different sets of specimens with different concrete compression strength tested under the impact loading that are applied by dropping constant weight hammer from five different heights. The acceleration arises from the impact loading is measured against time. The change of velocity, displacement and energy are calculated for all specimens. The failure modes of the specimens with normal and high concrete compression strength are observed under the loading of constant weight impact hammer that are dropped from different heights. Impact behaviors of beams are positively affected from the strengthening with CFRP. Measured accelerations, the number of drops up to failure and dissipated energy are increased. Finite element analysis that are made by using ABAQUS software is used for the simulation of experiments, and model gave compatible results with experiments.

Keywords: CFRP; low velocity impact behavior; strengthening; drop weight; ABAQUS

1. Introduction

Concrete is the most widely used construction material in the world. But concrete structural elements need retrofitting and strengthening due to different reasons. Some of these reasons cited as the change in structure usage need and loading, increase at loadings due to increase in needs, corrosion damages due to environmental effects, mistakes that are made during project and manufacturing phases. Due to these reasons or similar ones, there is a need for strengthening of concrete beams.

Strengthening techniques of concrete beams such as concrete jacketing, confinement with steel strips and many similar methods are investigated by the researcher up to now. But all of these techniques had many disadvantages such as increase in the weight of the member, affecting from corrosion and fire. In addition, they can not applied all of the members and require significant workmanship. For these

* Corresponding author, Ph.D., E-mail: oanil@gazi.edu.tr

reasons, Carbon fiber reinforced polymers (CFRP) is started to be used and became popular and widespread. CFRP is used widely due to lighter weight, resistant to corrosion and environmental conditions, ease of application to different and every type of surfaces and very high tension strength.

There are many analytical and experimental studies about the strengthening of beams by using CFRP against static loadings and dynamic cyclic loads such as earthquake or wind loads at literature. But authors encountered very limited amount of study about low velocity impact behavior of concrete beams. There are studies at literature that investigate the impact behaviors of concrete when the additive materials such polypropylene or steel fibers are added to concrete (Arslan 1995, Badr *et al.* 2006, Marar *et al.* 2001, Nataraja *et al.* 2005, Valipour *et al.* 2009). These studies showed that additive are affected the impact strength of the concrete positively. But these fibers made handling of the concrete different, increased the cost of it. In addition when the volume of the concrete increased, the homogeneous distribution of additives became difficult. As a result the properties of the concrete differ according to distribution. But there are limited amount of studies at literature about the RC beams strengthened with CFRP against the impact and blast loading (Muszynski 1998, Erki and Meier 1999). For these reasons, an experimental study conducted with the strengthened RC beams for the flexure against low velocity impact loading by using CFRP strips. Due to its nature impact loading is significantly complex type of loading. For this reason the behavior of concrete beams strengthened with CFRP strips under impact loading is also a complex and crucial subject, and it should be investigated. Although impact loads are not permanent and application properties (time, magnitude) are not known fully like the static loads, but instant magnitude can be larger than the other loading types (Krauthammer 1998, Magaraj *et al.* 1993, Goldsmith 1960, Murtiadi 1999).

There is no established standards or methods for impact testing up to nowadays' studies (Kishi *et al.* 2002, Ong *et al.* 1999, Mindess and Cheng 1993, Barr and Baghli 1988). But ASTM E 23 regulations improved the test setup performance significantly and gave good starting points for the limits of impacts experiments (Siewert *et al.* 1999). When the experimental impact studies at literature are investigated, they are categorized in to two main segments. One of them depends on the investigation on specimens under impact loads that are applied by test equipments. These types of studies are concentrated on mostly steel materials. The other studies use equipment with mechanisms that drop masses from height. This method is used mostly for the concrete impact testing (Banthia 1987, Bull and Edgren 2004). An impact tester that drops constant weight from a height is used for testing strengthened beams. This system is designed by the authors. A constant weight hammer is dropped from selected heights with low velocity and measured accelerations are investigated after the impact of free falling hammer.

Specimens with normal and high compression strength concrete are strengthened with widely used carbon fiber reinforced polymers (CFRP) in this experimental study. Different behavior under impact loading investigated. Totally ten rectangular cross section beam specimens are tested. Five of them are manufactured with normal and the other five with high compression strength concrete. All of them are strengthened with the same strengthening details by using CFRP strips, and are tested under free falling hammer with constant weight and geometry. Five different heights are tried such as 550, 600, 650, 700 and 750 mm. CFRP strip width and lengths are kept constant and the change in compression strength with the drop height are investigated in this experimental study. Velocity, displacement and dissipated energy values are calculated by using measured acceleration from the specimens. Specimens' strength, the number of hammer drop, acceleration values and failure mechanism are investigated, and the results of normal and high strength concrete specimens are compared. ABAQUS (ABAQUS user manual) finite element software is used for making simulation of the impact test at computer simulation environment. Results of the FEM are compared with experimental results for obtaining consistent finite

element model. As a results success of the FEM is investigated for the simulation of real experimental results, and the level of consistency of the results are determined.

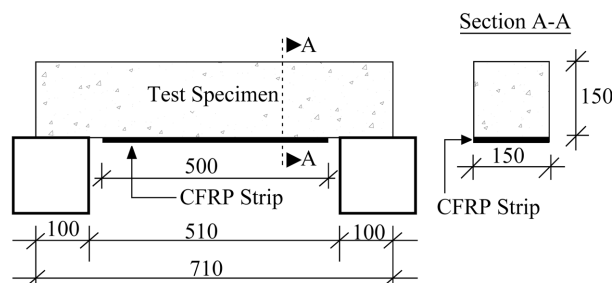
2. Experimental program

2.1 Test specimens and materials

Due to the fact that specimens are made up of concrete, free falling impact hammer test system is chosen for applying impact force. Geometric shape of the specimens, the material of the hammer and the shape of the hammer tip, the mechanical properties of the both specimens and strengthening materials are taken into account during preparation of the test methods. The factors that are affected on the behaviors of the concrete beam strengthened with CFRP are determined by making literature survey (Tang 2002). These factors can be cited as fallows; impact energy and initial velocity of the hammer, strain due to impact load, the type and weight of the composite material, the size of the bonding area of the composite, concrete compression strength, beam span, the bonding quality of the CFRP on to concrete surface.

All of the above parameters can not be investigated with a single study. Therefore some of them are kept constant during the experimental study. In this experimental study two different types of concrete compression strength, namely concrete with normal and high compression strength are investigated.

Beam specimens without reinforcements are manufactured for the experimental study with dimensions $710 \times 150 \times 150$ mm. Total 10 specimens at which half of them had normal and the remaining five had high strength concrete are tested. Impact loading is applied by using specially designed free falling hammer dropper. Constant weight is dropped from 5 different heights to specimens. Impact load is applied to specimens up to failure and behaviors of them are observed. Experiments are started from highest one and gradually height is reduced. Drop heights are 750, 700, 650, 600 and 550 mm. A first specimen with normal concrete compression strength is loaded with hammer that is dropped from 750 mm. Then for the second and the others drop height is reduced 50 mm. Fifth specimens is loaded with hammer dropped from 550 mm height. The same loading strategy is applied to specimens with high concrete compression strength specimens (Kantar 2009). Geometrical dimensions of the specimens with both normal and high concrete compression strength are the same and are given at Fig. 1. The other properties of the specimens are summarized at Table 1. Strengthening details of all specimens are the same. CFRP



Dimensions are in mm.

Fig. 1 Dimensions of test specimens

Table 1 Properties of test specimens

Specimen No	Specimen dimensions (mm)	Concrete compression		Weight drop height (mm)
		Capacity	Strength f_c (MPa)	
1	710 × 150 × 150	Normal strength concrete	28.4	750
2	710 × 150 × 150		24.8	700
3	710 × 150 × 150		30.3	650
4	710 × 150 × 150		27.6	600
5	710 × 150 × 150		25.3	550
6	710 × 150 × 150	High strength concrete	41.2	750
7	710 × 150 × 150		42.3	700
8	710 × 150 × 150		41.6	650
9	710 × 150 × 150		44.2	600
10	710 × 150 × 150		42.8	550

strips with the same geometry are bonded to face at which tension face is created when impact load applied. CFRP strips with single directional fibers (Sikawrap 230-c) are bonded to tension face of the beam by using the procedure suggested by the producer. Two component epoxy (Sikadur 330) is used for bonding 500 × 150 mm CFRP strips on to beams. Mechanical properties of the CFRP and the epoxy are given at Table 2. Beam tension faces at which CFRP strips are bonded roughened with mechanical grinder up to aggregates are exposed. Then these surfaces are cleaned with water soaked sponges, and are dried with compressed air. Two part epoxy is mixed up a point at which mixture took a uniform single color, then 0.5 mm thick epoxy is applied on to the surfaces, approximately. A special hand tool with 0.5 mm teeth is used for applying epoxy on to concrete surface. After that CFRP strips are laid on to epoxy by hand carefully without changing the directions of the fibers. Only single layer of CFRP is used for strengthening of specimens. As can be seen from the Table 2 of the manuscript, the thickness of the CFRP material is 0.12 mm. While making this, CFRP strips are soaked with epoxy without left any air bubbles between the beam surface and CFRP. Finally another 0.5 mm thick epoxy is applied on to CFRP strips for protecting the direction of the fibers. The explained strengthening technique is applied to all off the specimens identically. While applying the procedure, the attention paid on to temperature of the laboratories is around 20°C±2. When the epoxy is cured below 20°C, the curing time is elongated and epoxy is reached its final strength with more time. But also when the temperature is increased, curing time is decreased. 80°C is the upper limit for the temperature, after that epoxy lost its strength and can not be used. After CFRP strips are bonded, seven day curing time is passed for

Table 2 Properties of CFRP sikawrap 230-C (unidirectional) and resin sikadur 330

Properties of CFRP	Remarks of CFRP
Thickness (mm)	0.12
Tensile strength (MPa)	4,100
Elastic modulus (MPa)	231,000
Ultimate tensile strain (%)	1.7%
Properties of resin	Remarks of resin
Tensile strength (MPa)	30
Elastic modulus (MPa)	3,800

reaching the full strength of epoxy. After that specimens are tested.

The success of bonding of CFRP to concrete surface is strongly dependent on the proper application of the procedure and surface preparation. Keeping the direction of fibers of CFRP strips and soaking the epoxy into CFRP while avoiding air bubbles are the key factors for the success of bonding. Strengthening procedure should be done with great care for determining the impact behavior of strengthened specimen with CFRP strips completely (Anil and Belgin 2008, Anil and Belgin 2010, Anil *et al.* 2010, Baran and Anil 2010).

Concrete compression strength of the specimens is determined from axial compression test of standard cylindrical samples with 150×300 mm dimensions that are manufactured from the same concrete with specimens. Five specimens with normal concrete compression strength and other five with high strengths are casted in one day for obtaining close concrete compression strength. Compression strengths of the specimens are determined from the five samples that are taken from each specimen. The average results of the five cylindrical samples are given at Table 1 for each specimen. The correlations between the specimens from each type are very high. Specimens with normal concrete compression strength had 1.784 and 2.266 MPa variation and standard deviation, respectively. Variation and standard deviations values are very low, and are calculated as 0.854 and 1.171 MPa for specimens with high strength, respectively. Mixing ratios by weight for normal and high strength concrete are given at Table 3. Accurate manufacturing is done at laboratory environment for the high strength concrete. Plasticizer and silica fume that are mixed to high strength concrete is accurately weighted and they are mixed to water and cement before hand for homogeneous distribution. Besides due to extra care paid to manufacturing and preservation of the concrete, standard deviation and vitation became less at these high strength concrete.

Cylindrical samples of both specimens with normal and high concrete compression strength are cured under same cure conditions. They put inside a water tank after the day of casting and seven days later they are transferred to laboratory floor for resting 20 days. Samples of specimens with the same strength series are tested at the same day. Two types of aggregates are used with the diameters from 1 to 7 mm and 7 mm to 15 mm. KPC 42.5 Portland cement is used for concrete production. 1% and 10% plasticizer and silica fume are added to mixture by weight ratio of cement for obtaining high strength concrete, respectively. Sika® ViscoCrete® Hi-Tech 36 is used as a high performance hyper plasticizer and SikaFume®

Table 3 Concrete mix properties

Normal strength concrete		
Materials	Weight (kg)	Weight percentage (%)
Cement	22.5	20.9
Gravel (7-15 mm)	40	37.3
Sand (0-7 mm)	30	27.9
Water	15	13.9
High strength concrete		
Materials	Weight (kg)	Weight percentage (%)
Cement	42.3	18
Silica fume	4.23	1.8
Gravel (7-15 mm)	44.65	19
Sand (0-7 mm)	122.20	52
Plasticizer	0.48	0.2
Water	21.15	9

Table 4 Properties of plasticizer and silica fume

Plasticizer Sika® ViscoCrete® Hi-Tech 36	
Properties	Remark
Density	1.03-1.07 g/cm ³ , 20°C
PH value	3-7
Viscosity	26 cp, 20°C
Freezing point	-4°C
Solid particle percentage	23-27%
Chloride percentage dissolving into water	Max. 0.1%
Silica Fume SikaFume®-HR	
Properties	Remark
Density	0.65 ± 0.10 kg/l

HR silica fume is used as a powder additive to concrete in this study. Crucial properties of both additives are given at Table 4.

Specimens are strengthened with CFRP strips and are prepared for testing after completing their curing time. Specimens are painted with white plastic paint for observing the damage while experiments are made. After that places of sensors that are used for measuring impact loading effects of dropping hammer are determined and special brass apparatus are fixed on these places by using studs (Fig. 2(a)).

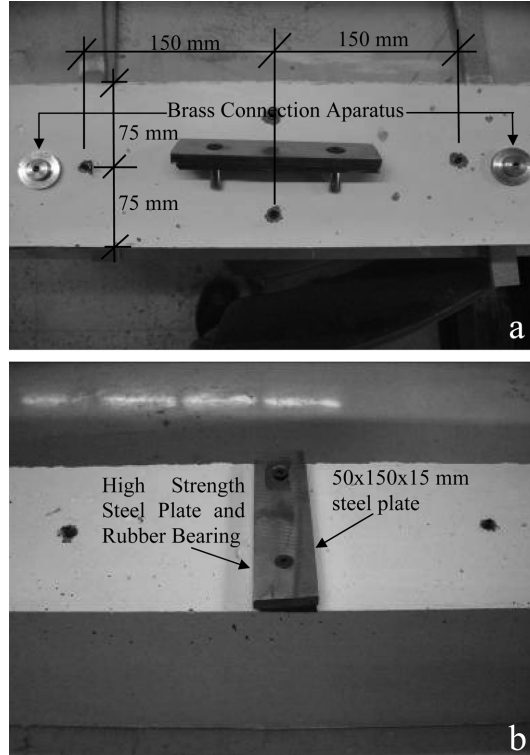


Fig. 2 Measuring devices preparation of specimens

In addition a specially manufactured steel plate with its silicone bearing is mounted with two steel studs on to region at which impact loading is applied with hammer (Fig. 2(b)). So loading is applied linearly all along the cross section. All of these apparatus are mounted on same locations, therefore identical loading is applied and measurements are taken. One of the specimens ready for testing looks like as shown in Fig. 3.

A different study is related to RC beams without strengthening by using CFRP strips that is done by Kantar *et al.* (2011a). This experimental study is conducted, and the effect of concrete compression strength variation on impact behavior of concrete investigated. Total ten beam specimens at which five of them are manufactured with normal compression strength concrete without reinforcement are prepared. Remaining five had high concrete compression strength. These specimens are tested under the impact loading that is applied by dropping constant weight hammer from five different heights. The acceleration due to impact loading is measured against time. The change of velocity, displacement and energy are calculated for all specimens. The failure modes of the specimens with normal and high concrete compression strength are observed under the loading of constant weight impact hammer that are dropped from different heights. The specimens that are tested at referenced study Kantar *et al.* (2011a) are the identical with the specimens of this study.

2.2 Test setup and instrumentations

The equipments in the literature that are used for dropping hammer are designed such that they allow to drop hammers with different weight from adjustable heights. By the help of investigated studies the dimensions of the equipment are determined. The most significant parameter that is effective on the result of impact test is the eccentricity. By the help of pre drop tests, eccentricity is minimized. During these tests, the weight of the base of test equipment is increased, and as a result, eccentricity is became zero. The detail of the designed equipment is shown in Fig. 4. The base is manufactured from square 1,000 mm by 1,000 mm steel plate that weight about 1,000 kg. Due to the fact that specimen sizes can change, the platform of the test equipment is manufactured as large as possible. Experimental setup has the capability of dropping variable weights from 2500 mm. Existing hammer weight can be increased by adding extra weights for the different experimental purposes. The weight of the hammer is 5.25 kg and same hammer is used for all experiments. Drop height is changed between 550 mm to 750 mm. The other effective parameter on the test result is known as friction, and friction is reduced by using

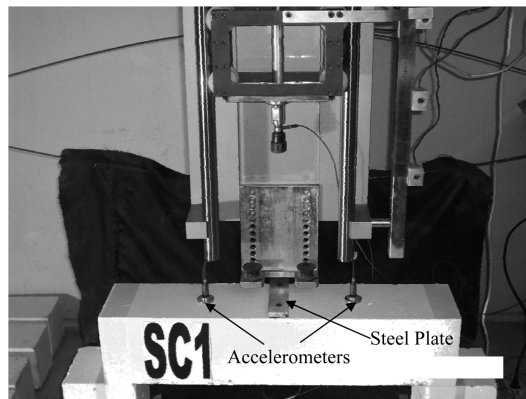


Fig. 3 Specimen 1 before Test

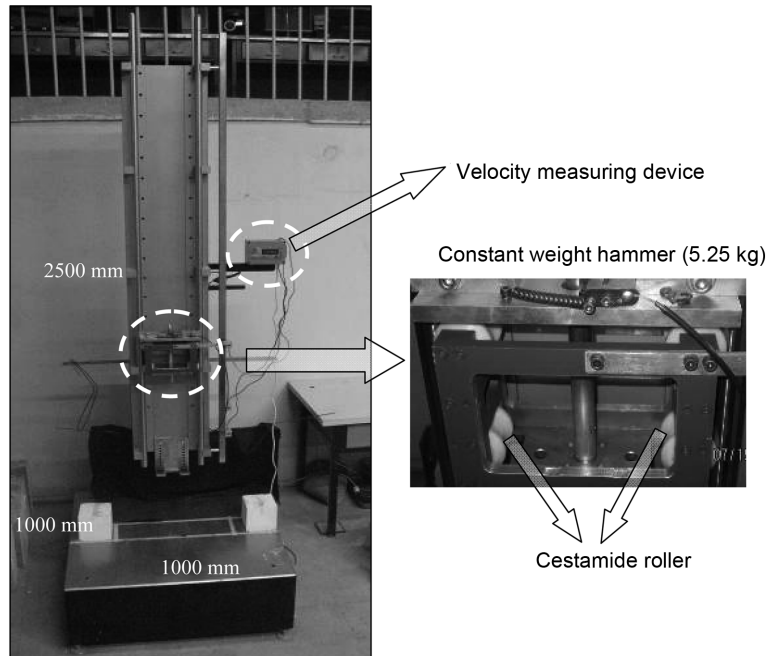


Fig. 4 Test setup

special materials. Hammer is guided with hard chrome coated grinded rods and cestamide rollers are used between the hammer and the rods during free fall.

Hammer first hit to a steel plate that is supported with a rubber cushion. The purpose of using steel plate is to distribute the load linearly and uniformly to the cross section of the specimen. For minimizing the internal forces, hard rubber is used between the specimen and steel plate. The dimension of the steel plate and rubber are $50 \times 150 \times 15$ mm. Steel plate with rubber is fixed to specimen by using steel dowels (Fig. 2). An instrument is placed along with the setup for measuring the terminal velocity of the hammer. Instrument uses optical photocells for measuring the drop time and from the time velocity can be calculated.

Two accelerometers are mounted on symmetry axis of the specimen, and 150 mm apart from the center of symmetry. Right and left side of the specimen and difference between them are measured with these two accelerometers. Accelerometers are mounted on brass apparatus that are mounted on to specimen by using steel dowels (Fig. 2). The data from accelerometers are transmitted to a data logger that is connected to computer and then analyzed with software.

3. Test result and discussions

3.1 Observed behavior and failure modes of specimens

Impact loading is applied to specimens from 5 different heights up to failure by using constant weight (5.25 kg) hammer. Internal effects after each drop are measured with accelerometers. Crack initiation and propagation, the number of the hammer drop, acceleration-time relation and specimens' general behaviors are observed during the experiments. The changes of drop heights with the number of drops

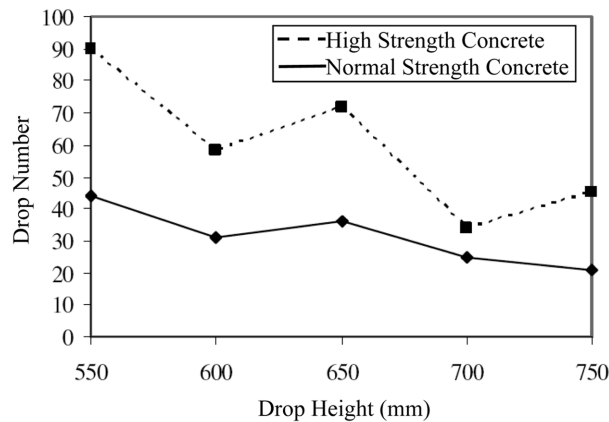


Fig. 5 Drop height-drop number relation of specimens

are given in Fig. 5. As the drop height is increased, the total number of drops is decreased for both normal and high compression strength concrete specimens strengthened with CFRP strips. Decrease in the total drop number is quicker at high strength specimens than the normal strength ones, when the drop height increased. The total number of drops up to failure is very close for the high and normal compression strength concrete when the drop high is increased up to 700 and 750 mm. Drop numbers is affected from compression strength of concrete but also are affected from tensile strength and fracture toughness of concrete. Authors thought that increase in the drop height also increase the applied energy, and this causes to number of drops before reaching to failure are became close for both normal and high compression strength concretes. Although compression strength of the concrete is increased, applied impact energy increase with drop height is caused to become approximately close number of drops up to failure for both types of specimens. For these reason as the drop height increased the number of drop at which failure occurred became close to each other. Drop time is measured with optical photocell at experimental setup and there is a relation between drop time and height only. Concrete compression strength has no effect on drop time. Drop time and the number of drop at which first and total damage is observed are given at Table 5 for all specimens.

The damage styles and failure modes are differ for the normal and high strength concrete compression

Table 5 Total drop number, first damage drop number and drop time of specimens

Spec. #	Drop height(mm)	Drop time(ms)	Total drop number	First damage drop number	
1	750	498.00	21	6	
2	Normal strength concrete	700	471.00	25	12
3		650	445.00	36	11
4		600	419.00	31	20
5		550	393.00	44	36
6		750	498.00	45	30
7	High strength concrete	700	471.00	34	19
8		650	445.00	72	47
9		600	419.00	58	29
10		550	393.00	90	79

strength specimens that are strengthened with CFRP strips. Due to the fact that the ductility of the normal strength specimens are larger than the high strength ones, the number of the hammer rebound is less than the high strength specimens. Authors though that, normal concrete is attenuated the impact load quicker than the high strength concrete due to higher ductility. The numbers of rebounds are changing according to drop heights, but the time passing between rebounds is not affected. This is an indication of all specimens have similar concrete strength.

As can be seen from the acceleration measurements that are taken from specimens, the number of rebounds are more at the initial drops at which limited damage it observed than the number of rebounds at later drops as the number of drops increase. This is the indication of increase in the number of internal hair cracks that are not visible with naked eye, when the numbers of drops are increased. Sample graphs for Specimen 3 and 8 that show the change of the number of rebounds and time between rebounds versus the number drops are given at Fig. 6. As the numbers of drop are increased, rebounds are decreased. Increase at the amount of damage is caused to decrease at the number of rebounds. The time of rebounds are decreased with the effects of increase in damage. The amount of dissipated energy and the time between two rebounds is decreased, while the damage was increasing. The rebounds are last shorter and the hammer became stationary sooner with the increasing damage. This observation is valid for both standard and high strength concrete specimens. Appearance of visible cracks and propagation of cracks are observed at specimens with normal concrete at earlier drops than the ones with high strength concrete. Cracks are initiated at the upper face of the both specimen series and are propagated towards the face at which CFRP bonded. An opposite crack initiation and propagation scheme is observed at the specimens at which no CFRP strengthening is applied (Selvi 2008, Kantar *et al.* 2011 a). The number of drops that is required for initial damage and failure are increased significantly at the strengthened specimen with CFRP, when compared to specimens without strengthening. Failure modes are also significantly different at strengthened specimens. Sudden failures are observed at the specimens without strengthening and failure surfaces at which cracks are initiated are completely separated. As a result specimens are lost their stability and are separated in to two pieces. In contrary strengthened specimens with CFRP are not lost their stability, although failure plane is completely formed and

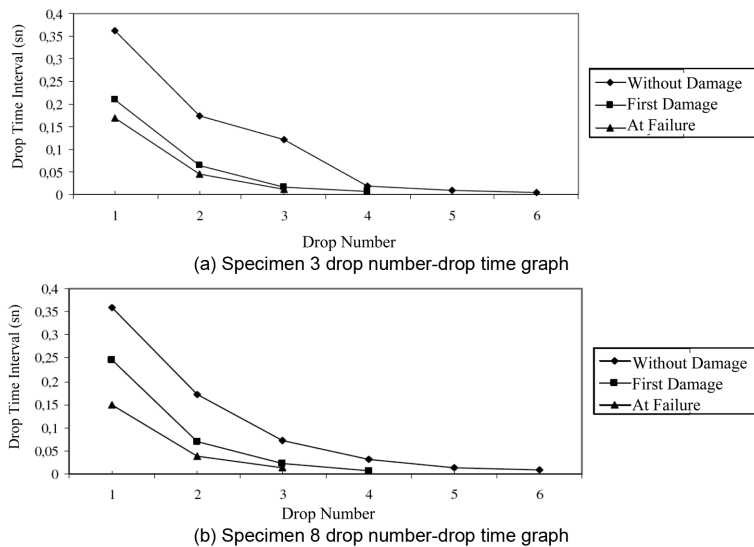


Fig. 6 Drop number- drop time interval relation of specimens

specimens are separated in to two parts.

CFRP strips prevented the stability lost without debonding from surface, and specimens did not failed completely. Although aggregate and matrix is separated, CFRP epoxy and concrete layer did not separate. Specimen 3 and 8 are the specimens that are tested by dropping hammer from 650 mm, and Specimen 3 is manufactured with normal strength concrete, where as Specimen 8 is manufactured with high strength concrete. The Figs. 7 and 8 are taken after failure of the Specimens 3 and 8, respectively. When the failure plane of the specimens with normal concrete are investigated, the failure is occurred between the surfaces of aggregate and matrix. There is no broken aggregate. A picture that is taken from the failure plane of Specimen 3 one of the normal strength concrete specimens is given in Fig. 9. When the failure planes of

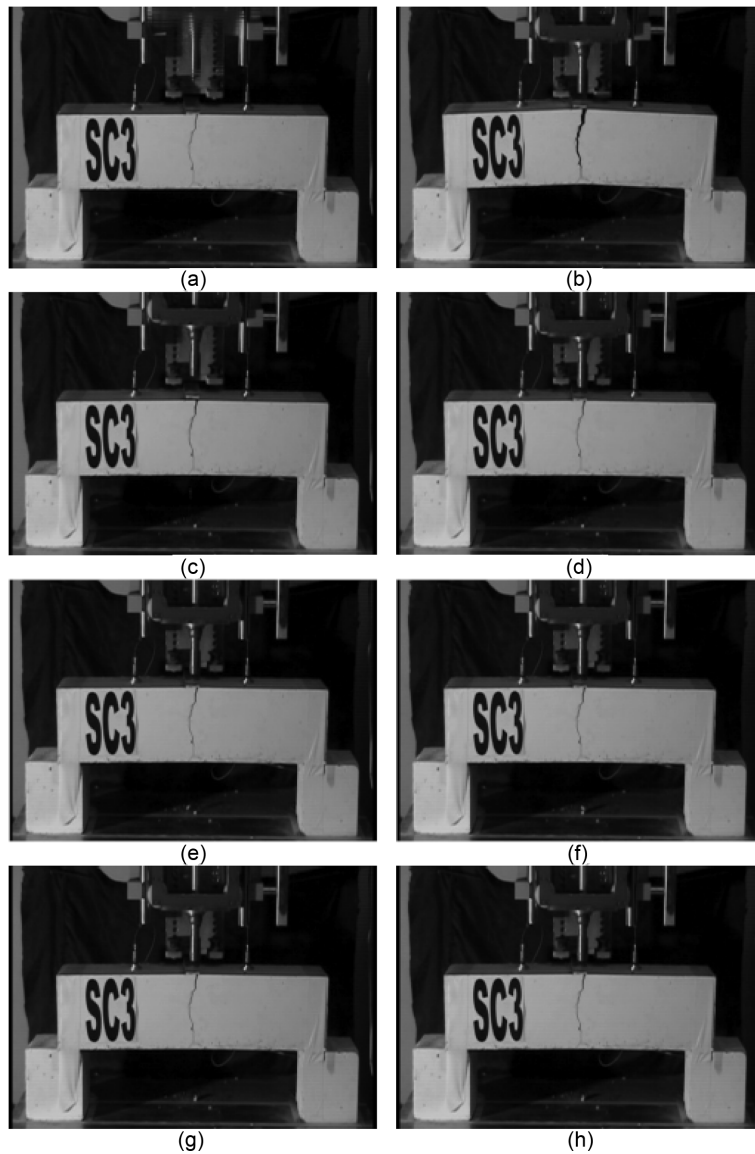


Fig. 7 Failure drop cycle of specimen 3

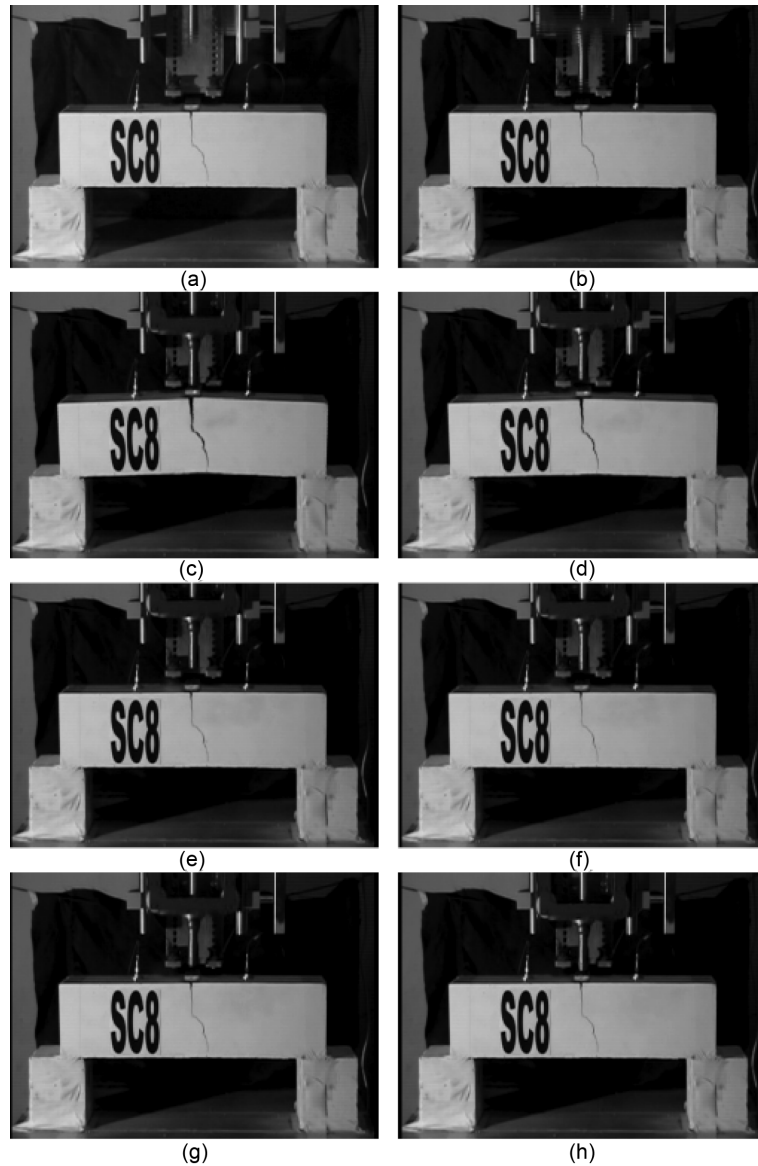


Fig. 8 Failure drop cycle of specimen 8

the specimens with high strength concrete are investigated, the failure plane is occurred by cutting both aggregate and matrix and picture of one of the failure plane is given at Fig. 10 as an example.

Specimens are stayed stationary during impact and impact point did not change up to failure. There is no stability problem up to last drop at which failure is occurred. A steel apparatus from high strength steel is used at the mid point of the beam for transferring loading along a line exactly to mid point at each drop. Due to high weight of beams and supports no jerking or instability is encountered during testing. Therefore no energy is lost and all of them are transferred to beam. CFRP strips are not peeled from the surface and specimens are divided into two pieces with the failure plane, CFRP strips are preserved the completeness and stability of the specimens.

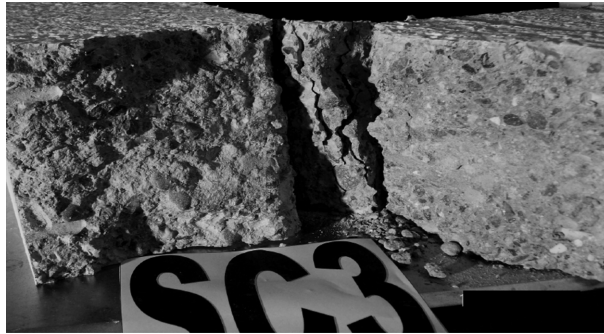


Fig. 9 Failure plane of specimen 3

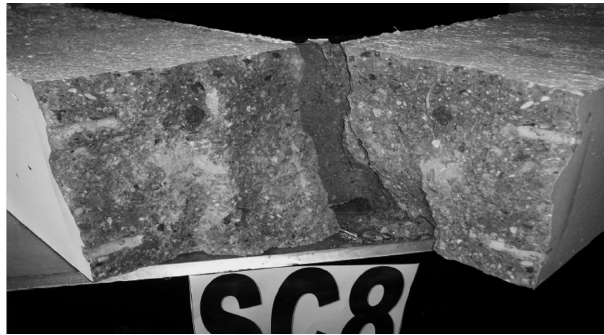


Fig. 10 Failure plane of specimen 8

3.2 Acceleration, Velocity and Displacement Behaviors of Specimens

Two symmetrical acceleration measurements are taken from the beam for determining internal behaviors against impact loading. Time dependent velocity and displacement graphs are obtained by using acceleration graphs. Velocity and displacement are calculated by taking integration of the acceleration with time. Specimen 3 with normal strength concrete maximum acceleration, velocity and displacement graphs are given in Fig. 11 as a sample. Same graphs for the high strength concrete Specimen 8 is presented at Fig. 12. The values for the maximum and minimum accelerations, velocities and displacements, when the first drop without damage, first damaged observed drop and failure drop are summarized at Table 6. First damage is observed by eye after each drop. Drop at which first capillary crack is observed at the upper side of the beam is named as first damage drop. Failure drop is defined as the drop at which failure plane is reached to bottom of the beam. As a result, the concrete cross section of the beam is divided into two pieces with the failure plane but CFRP strip is not ruptured and is preserved the stability of the strengthened beams.

After the first interaction of the hammer with the specimen, a downward acceleration like the gravitational acceleration is observed and this acceleration creates a downward deformation. As can be seen from the displacement graphs, deformation took a negative value at the beginning, but this value remain very small at the undamaged drop, first damage and failure states of the specimens. This displacement increased a little up to failure plane formation. Due to strengthening with CFRP at tension face of the specimens. Specimens tried to move opposite direction to impact direction of the hammer. This can be

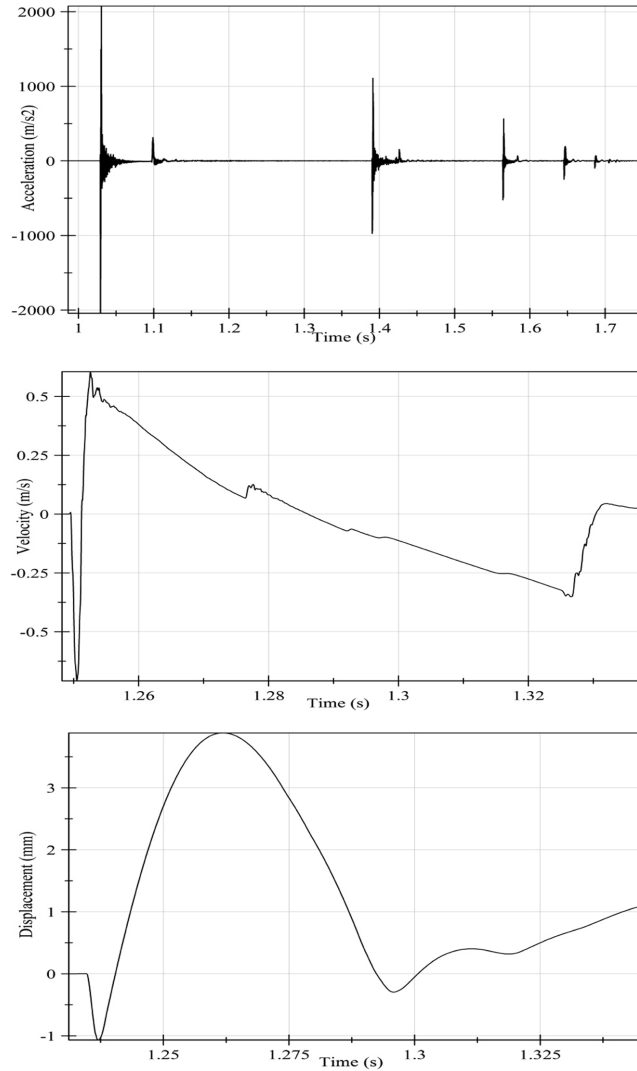


Fig. 11 Maximum acceleration, velocity and displacement graphs of specimen 3

seen from the camera pictures and the deformation graphs.

Due to damping effect of the hammer, an opposite directional acceleration is measured with each rebound of the hammer from the beam surfaces. When acceleration-time graphs are investigated, the number of the rebounds and the acceleration values are appears to be different for each specimens. This finding showed that the material is not homogeneous, and different capillary internal cracks are formed for each specimen with hammer drops. In general, like acceleration time graphs, a velocity time graphs are also showed changes at each rebound. First velocity is increased with the same direction of deformation, and then when the interaction of the hammer with the specimen is finished, the specimen is returned its original position with increasing velocity in the opposite direction. But when the velocity-time graphs of failure drops are investigated, all of the velocity increases are became in same direction with the failure. Velocities are decreased with the decrease in energy transferred to specimens

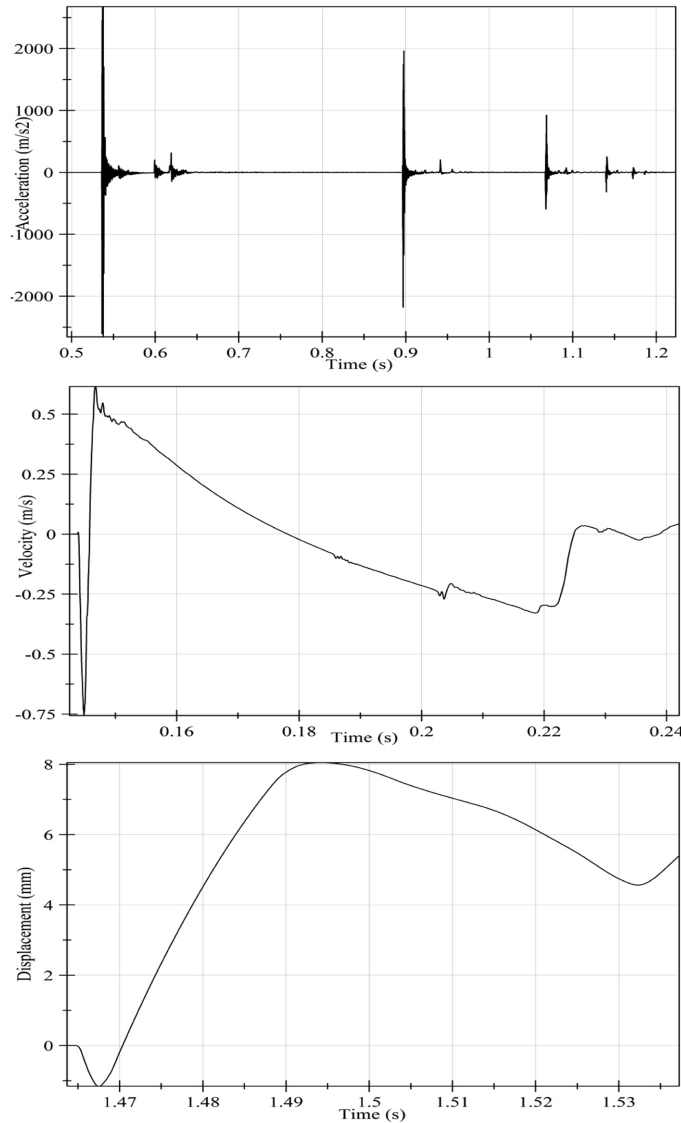


Fig. 12 Maximum acceleration, velocity and displacement graphs of specimen 8

from the hammer, and acceleration. Like in acceleration-time graphs, amplitude of the velocities is not symmetrical at velocity-time graphs.

3.3 Absorbed energy capacities of specimens

It is assumed that all of the potential energy lost by the hammer during drops is transferred to internal deformation energy of strengthened specimens with CFRP while calculating specimens' energy capacities and no energy lost is occurred. In addition, linear elastic material assumption is made during calculations, and uncracked moment of inertia is used. While calculating the stored deformation energy of the

Table 6 Experimental results

		First drop			First damage drop			Failure drop		
		Acceleration (m/s ²)	Velocity (m/s)	Displacement (mm)	Acceleration (m/s ²)	Velocity (m/s)	Displacement (mm)	Acceleration (m/s ²)	Velocity (m/s)	Displacement (mm)
SC1	Min.	-2725.02	-0.69	-0.06	-2205.39	-0.73	-0.77	-2441.91	-0.87	-1.66
	Max.	2719.63	0.41	4.65	2679.41	0.55	6.52	2727.77	0.34	487
SC2	Min.	-2352.54	-0.63	-0.50	-2345.57	-0.76	-1.04	-2600.83	-0.90	-1.33
	Max.	2716.19	0.48	5.30	2501.35	0.66	9.01	2450.05	0.37	4.22
SC3	Min.	-2705.70	-0.61	-0.55	-2405.31	-0.70	-0.73	-2284.65	-0.73	-1.06
	Max.	2631.34	0.50	5.66	2649.39	0.60	7.21	2535.59	0.43	3.88
SC4	Min.	-1592.56	-0.41	-0.30	-2154.77	-0.82	-0.68	-2724.34	-0.83	-12.21
	Max.	2547.17	0.37	2.58	2473.89	0.68	8.31	2727.28	0.50	4.93
SC5	Min.	-1535.76	-0.65	-0.57	-1556.36	-0.75	-9.66	-2725.02	-0.85	-23.82
	Max.	2655.27	0.49	4.51	2678.13	0.52	5.24	2728.06	0.19	0.00
SC6	Min.	-2686.76	-0.30	-0.22	-2071.58	0.40	-0.29	-2677.35	-0.68	-1.08
	Max.	2728.06	0.84	28.42	2522.05	1.04	30.47	2728.06	0.69	13.20
SC7	Min.	-2586.11	-0.56	-0.42	-2588.96	-0.22	-0.17	-2717.47	-0.37	-0.49
	Max.	2648.90	0.53	4.34	2533.14	1.07	41.6	2668.42	0.87	27.15
SC8	Min.	-2725.02	-0.37	-11.49	-2656.74	-0.75	-1.42	-2725.02	-0.70	-1.15
	Max.	2728.06	0.49	4.32	2616.52	0.61	7.49	2678.13	0.57	8.04
SC9	Min.	-2441.81	-0.53	-1.13	-2031.06	-0.72	-0.86	-2649.78	-0.71	-15.10
	Max.	2320.36	0.44	2.45	2480.56	0.53	3.79	2568.26	0.27	0.93
SC10	Min.	-2574.34	-0.30	-0.20	-2549.32	-0.36	-0.26	-2643.21	-0.33	-0.39
	Max.	2648.70	0.56	6.35	2592.29	0.66	7.35	2525.00	0.66	27.27

specimens, energy that is stored by the influence of bending moment is taken into account, and energy that is formed due to shear forces is neglected. Displacement profile is assumed to be sinusoidal and given at Eq. (1)

$$u(x, t) = u_0(t) \sin\left(\frac{\pi x}{l}\right) \quad (1)$$

Eq. (4) is obtained by putting the kinetic energy, and bending energy equations that is given at Eq. (3) into energy equilibrium equation that is given at Eq. (2) (Kishi *et al.* 2002).

$$\Delta E_0(t) = T(t) + U(t) \quad (2)$$

$$T(t) = \frac{\rho B D l}{4} \dot{u}^2(x, t) \quad (3)$$

$$\Delta E_0(t) = \frac{\rho B D L}{4} \dot{u}^2(t) + \frac{\pi^4 E I}{4 l^3} u_0^2(t) \quad (4)$$

Table 7 Comparison of experimental and finite element model acceleration and energy capacity of specimens for measured maximum acceleration drop cycle

Spec No.	Acceleration (m/s^2)				Experimental/ ABAQUS Acceleration Ratio		Energy (J)		Experimental/ ABAQUS energy ratio
	Experimental		ABAQUS		Maximum	Minimum	Experimental	ABAQUS	
	Maximum	Minimum	Maximum	Minimum					
1	2719.63	-2725.02	2461.98	-1395.74	1.10	1.95	5.16	5.14	1.00
2	2716.19	-2352.54	2523.38	-1924.74	1.08	1.22	5.66	4.90	1.16
3	2631.34	-2705.70	2535.18	-1732.07	1.04	1.56	4.81	5.07	0.95
4	2547.17	-1592.56	2462.72	-1461.01	1.03	1.09	6.55	4.74	1.38
5	2655.27	-1535.76	2063.14	-1552.69	1.29	0.99	4.06	3.32	1.22
6	2728.06	-2686.76	2636.99	-1543.64	1.03	1.74	10.40	5.54	1.88
7	2648.90	-2586.11	2494.12	-1466.10	1.06	1.76	11.16	5.04	2.21
8	2728.06	-2725.02	2221.02	-1381.45	1.23	1.97	5.48	4.19	1.31
9	2320.36	-2441.81	2274.01	-1649.27	1.02	1.48	5.03	2.65	1.90
10	2648.70	-2574.34	2198.09	-1246.71	1.21	2.06	4.28	4.02	1.06

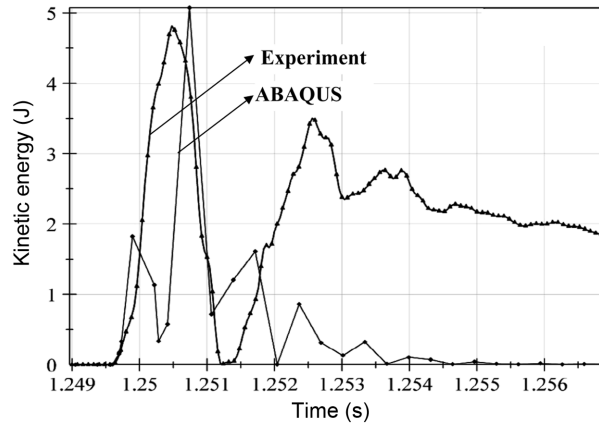
Velocity values that are obtained from the measured accelerations are used in Eq (3) for calculating kinetic energies. Bending energy that is calculated by assuming sinusoidal deformation profile is added by kinetic energy for obtaining total experimental measured energy. Absorbed energies that are calculated for specimens with normal and high concrete strength are presented in Table 7 for the drop at which maximum acceleration are measured. In addition analytical and experimental absorbed energy graphs for the Specimen 3 with normal and Specimen 8 with high concrete strength are given at Fig. 13 for comparison. Finite element analyses are used for obtaining the graph at drops which maximum acceleration is measured. Average calculated energy values for the specimens with normal concrete strength is 29% smaller than that of specimens with high concrete strength except the Specimen 4 for the drop at which maximum acceleration is measured. The difference between the observed energy capacities increased as the drop height increase. The difference between the normal and high strength series reached the highest value at the 750 mm drop height.

4. Analytical study

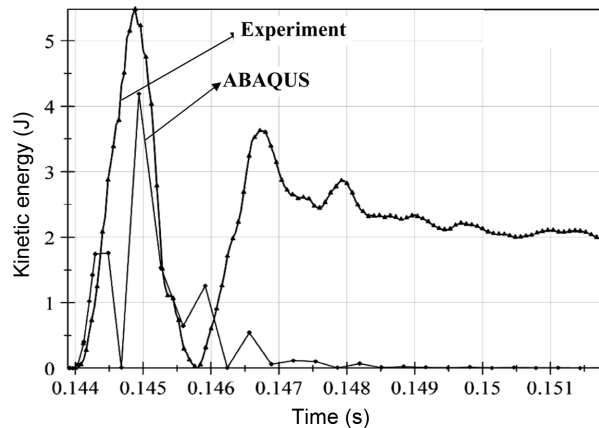
4.1 Finite element modeling of experiment

Investigated literature emphasized that generalization of the results can be done if large number of experiment are done, and the large amount of data is required for this purpose. But the design of the laboratory test system and specimens took time and required lots of investment. For these reasons authors though that a finite element model that is verified with experimental results can gave a preliminary idea for designer, and became helpful. For this purpose, a simulation is done by using ABAQUS finite element software for the investigated experimental study. The FEM and experimental results are compared and the level of consistency between them is investigated.

ABAQUS software is used for FEM modeling in this study, due to its properties such as dynamic modeling capability, ease of 2D and 3D modeling, and availability of variety of elements types with different material models in the library. Linear-elastic material model is used for the modeling of CFRP,



(a) Experimental and finite element model energy capacity graphs of specimen 3



(b) Experimental and finite element model energy capacity graphs of specimen 8

Fig. 13 Comparison of experimental and finite element model energy capacity for specimen 3 and specimen 8 at maximum acceleration drop cycle

specimen and the hammer. Impact loading is a dynamic loading; therefore loading is started from a small magnitude and with small time increments increased up to its final value nonlinearly. Impact required a time dependant nonlinear simulation due it is nature. Impact analyses require small time steps and transfer of load at the moment just the hammer touch to the specimen. For these reasons, an impact analysis requires extensive computer time and capacity. Some simplifications are made for making analyses of all of the specimens. For these reasons nonlinear behavior of concrete and CFRP-concrete contact problems are neglected in this studies' model. Authors are concentrated onto impact modeling and are neglected nonlinear behavior of concrete. (Kantar *et al.* 2011b). The dimensions of the specimen, setup and supporting condition are modeled like in the experimental study. Snap shot of the FEM mesh is given in Fig. 14. While the size and refinement of the FEM mesh is determined, a finite mesh size is chosen and then refinement is done up to reaching a threshold between the results of two consecutive runs. Mesh density is increased up to a level at which the acceleration and displacement values are became very close after consecutive two runs. Then this mesh density is used for the remaining analyses. If the results of two run is close enough, refinement is stopped. The experimental and FEM results such as acceleration and energy absorption values, stress distribution and failure

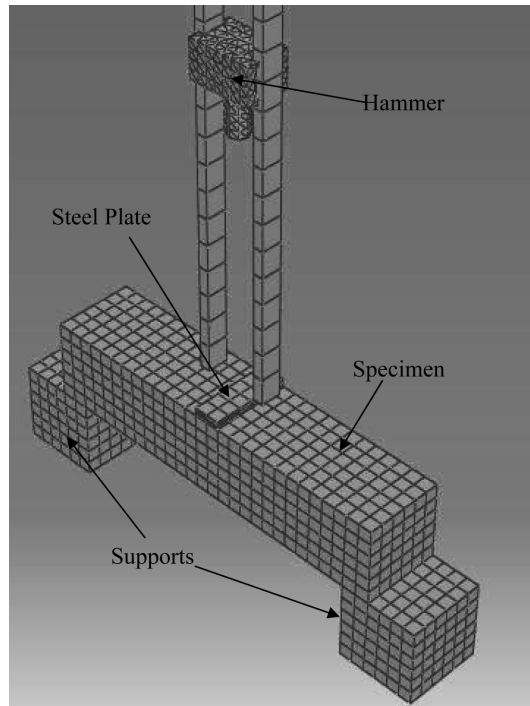


Fig 14. Finite element mesh of specimens

modes are compared.

Acceleration graphs that are obtained from experiments and FEM analyze for Specimen 3 with normal strength concrete and Specimen 8 with high strength concrete is given at Fig. 15 for comparison. When the graphs are investigated, both results are seemed to be consistent with each other. But as can be seen from Table 7, there is 9% and 33 % difference between experimental and FEM result at maximum and minimum acceleration value, respectively. Authors thought that this difference between acceleration values can be due to linear elastic material model that is used for CFRP, and assumption that are made during impact modeling and concrete element. In addition, stress distribution graphs that are obtained from FEM modeling and experimental damage and failure planes are compared. Stress distributions that are obtained from FEM analyses for Specimen 3 with normal strength concrete and Specimen 8 with high strength concrete are given at Fig. 16. FEM analyses are made for the case at which hammer is dropped from 650 mm. When the stress distribution graphs of FEM analyses are investigated, after the impact is occurred a sudden stress concentration is observed and this residual stress is remained on to the specimen. Due to differences at the elastic modulus of the materials, the stress at the hammer is significantly larger than the stress at the specimen. A crack line is observed at the specimens due to cyclic application of stress concentration that is created by the impact loading. Experimental damage and crack lines are showed similarities with the ones that are obtained from FEM. Damage and failure plane at experiments are occurred at the regions where stresses are concentrated. Especially the failure planes of specimens with high strength concrete are more consistent with FEM analyses than the specimens with normal strength concrete.

During finite element modeling, nonlinear material behavior of concrete and nonlinear time dependent change due to contact between CFRP and concrete are neglected. Linear elastic material

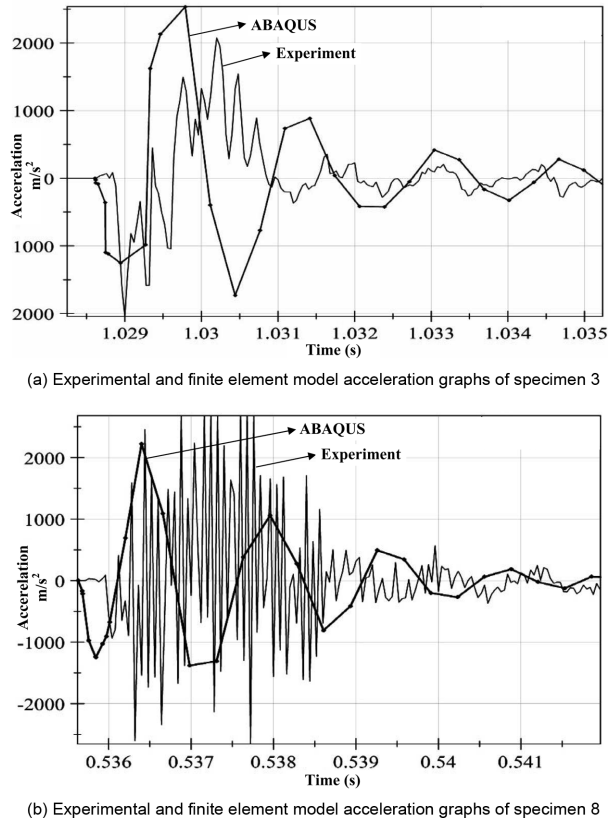
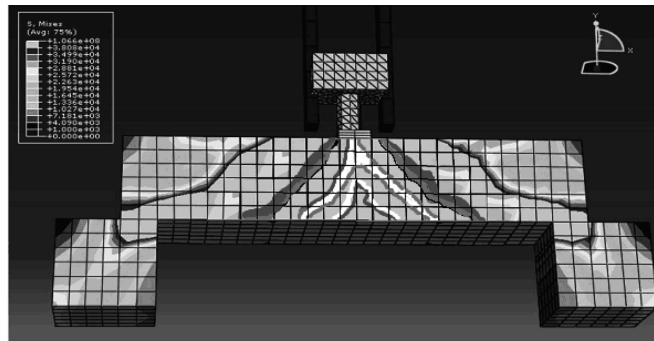


Fig 15. Comparison of experimental and finite element model acceleration for specimen 3 and specimen 8 at maximum acceleration drop cycle

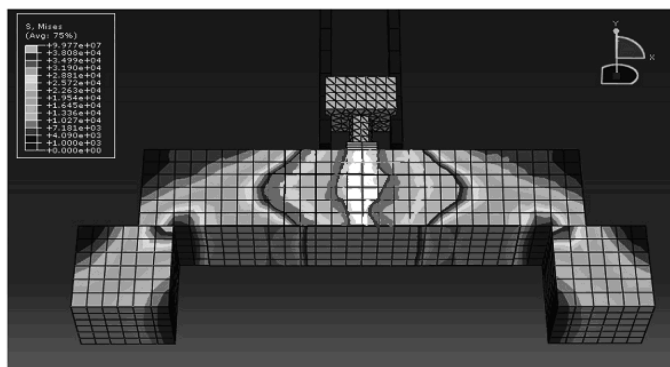
model is used for concrete, and CFRP is assumed as fully bonded to concrete instead of using special contact elements between them. Small time increments are required for correct modeling of nonlinear-dynamic impact behavior. For this reason, completing computer analyses are took too much time. Same model is solved for every small time increment for simulating impact. For these reasons, nonlinear parameters such as concrete material properties and CFRP-concrete contact are not included in the analyses for reducing the runtime. Calculated FEM energies are evaluated by using linear-elastic materials models. As can be seen from the Table 7 the difference between the experimental and FEM energy dissipations can be 23% in average. This difference stems from the usage of the linear elastic material model instead of anisotropic and non homogenous concrete, and assumptions that are made at the energy calculation can not simulate the elasto-plastic real impact situation sufficiently.

5. Conclusions

The purpose of this study is to investigate the behavior of strengthened RC beams with CFRP strips under the low velocity impact loading that is applied by the free fall of hammer. The investigated parameters are the drop height of the constant weight and concrete compression strength. Specimens



(a) Stress distribution contour of specimen 3



(b) Stress distribution contour of specimen 8

Fig 16. Stress distribution contour for 650 mm drop height

with two different concrete compression strengths are tested with dropping hammer from five different heights. Identical strengthening details are applied to all of the specimens. Evaluations that are made after experiment can be cited as the number of drop that causes failure, acceleration, velocity, displacement, time, energy capacities, crack arrangement and propagations. In addition simulation of the experimental study is made under the light of the obtained result by using FEM software. Widely used ABAQUS FEM software is used for its dynamic modeling capability in this study. FEM and experimental results are compared, and the consistency of the FEM to experimental results is investigated. The results of this study can be cited below as follows;

- The behavior of the concrete, which is widely used in the world as a construction material, against impact loading is not known well and there is no standard test procedure for this loading type. Due to limited amount of experimental data and lack of standard test procedure, generalization became very hard. Nowadays strengthening and retrofitting became widespread, and CFRP fabrics are started to be a used for strengthening and retrofitting of RC structures. Lots of studies about these materials are made and effects on dynamic and static characteristic of concrete are investigated. But authors did not encounter any study about behavior of strengthened RC beam with CFRP against low velocity impact loading in literature. For these reasons experimental results that are observed from this study are crucial. Widely used free falling hammer experimental setup is preferred for applying impact loading.
- Success and quality of the bond between CFRP and concrete is affected on the impact behavior

significantly. If bonding between CFRP and concrete can not provided at required level, CFRP is peeled from the concrete surface at the early drops. But in this study, peeling from the surface is not observed at any of the tests. Although concrete beams that are manufactured from both normal and high strength concrete are divided into two pieces, CFRP strips are not peeled from the surface and are preserved the stability of the specimens.

- The numbers of drops up to failure are compared as a result of experiments. The number of drops is changing nearly linear manner with respect to drop height and concrete compression strength Specimen 4 with normal concrete strength and Specimens 7 and 9 with high concrete strength did not obeyed this linear behavior. One of the main reasons of this thought to be the non homogeneous characteristics of the concrete. Non homogeneous distribution of aggregate and the interaction between aggregate and the other thin matrix materials ruined the similarity of the specimens. In addition, although same strengthening details are applied to specimens, small differences can cause change in behavior.
- The number of rebound changed with respect to drop height, but the time between two consecutive rebounds appeared to be same. This showed that the concrete properties for each series of specimens are very close. The numbers of rebounds are high at first drops, and reduced at the cycle at which first damage observed, and then the least number of rebounds are observed at cycles which failure plane is formed. These findings showed that when the numbers of drops are increased, internal damage and cracks are increased. The numbers of drops are decreased faster at specimens with normal concrete compression strength than the specimens with high strength. This can be due to faster internal damage occurred at specimens with normal concrete strength.
- Cracks became visible from outside with increasing number of drops and started from upper side. Then propagated towards to face at which CFRP strengthening is applied. An opposite crack scheme is observed at specimens at which no CFRP strengthening is applied. The number of drops that is required for initial damage and failure are increased significantly at the strengthened specimens with CFRP, when compared to specimens without strengthening. Failure modes are also significantly different. Sudden failures are observed at the specimens without strengthening and failure surfaces at which cracks are initiated are completely separated. In contrary strengthened specimens with CFRP are not lost their stability, although failure plane is completely formed and specimens are separated into two parts. Although aggregate and matrix is separated at all strengthened specimen with CFRP, CFRP epoxy and concrete layer did not separate.
- When the failure planes of the specimens with normal concrete are investigated the failure is occurred between the surfaces of aggregate and matrix. Specimens with high concrete compression strength failed by cutting both aggregate and matrix without separation due to high density of thin materials.
- When acceleration-time graphs are investigated, increase in number drops caused to increase in invisible damages. As a result of the conversion of potential energy of the hammer to kinetic energy, these damages became permanent. According to material structure and the number of drops, specimens reached to failure passing from elastic state to plastic one. After the first interaction of the hammer with the specimen, a downward acceleration like the gravitational acceleration is observed and this acceleration creates a downward deformation. As can be seen from the displacement graphs, deformation took a negative value at the beginning, but this value remain very small at the undamaged drop, first damage and failure states of the specimens. This displacement increased a little up to failure plane formation. Due to strengthening with CFRP at tension face of the specimens. Specimens tried to move opposite direction to impact direction of the hammer. This can

be seen from the camera pictures and the deformation graphs.

- Acceleration-time, velocity-time and displacement- time graphs that are obtained from ABAQUS FEM software are compared with experimental results. Non homogeneous, anisotropic and nonlinear concrete elements are needed for the modeling of concrete specimens. CFRP strips are modeled as fully bonded and the interface surfaces are not modeled by using special contact element. Impact is modeled as nonlinear dynamic analyses with great care.
- When acceleration graphs that are obtained from FEM are investigated, general behavior and the maximum values are fit quite well with the experimental results. But analyses results are consisted of quite a few points, therefore only the maximum jump and general appearance are fit. The number of rebounds that are obtained from experiments and FEM analyses are quite similar.
- Nonlinear concrete elements are cracking at tension and crushing at compression is modeled as linear elastic. Due to modeling of CFRP strip concrete interface as a rigid connection and neglecting interface parameters, specimens' models are behaved more rigid than the real ones. Failure planes that are obtained from the tests are consistent with the stress distribution contours that are obtained from FEM analyses. The regions at which stress concentrations are observed, damage occurred and failure plane formed.
- Specimens that are manufactured from high compression strength concrete are dissipated more energy that the ones with normal strength.

References

ABAQUS/Explicit User Manual, Version 6.7.

- Anil, Ö. and Belgin, Ç. (2008), "Review of bond-strength models and application on CFRP to-concrete bonded joints across crack", *Science. Eng. Comp. Mater.*, **15**(2), 141-158.
- Anil, Ö. and Belgin, Ç. (2010), "Anchorage effects on CFRP-to-concrete bond-strength", *J. Reinforced. Plastics. Comp.*, **29**(4), 539-557.
- Anil, Ö., Belgin, Ç. and Kara, M.E. (2010), "Experimental investigation on CFRP to concrete bonded joints across crack", Techno Press, *Struct. Eng. Mech.*, **35**(1), 1-18.
- Arslan, A. (1995), "Mixed-Mode fracture performance of fibre reinforced concrete under impact loading", *Mate. Struc.*, **28**, 473-478.
- Baran, A. and Anıl, Ö. (2010), "Nonlinear finite element analysis of effective CFRP bonding length and strain distribution along concrete-CFRP interface", Techno Press, *Comp. Concrete. Inter. J.*, **7**(5), 427-453.
- Badr, A., Ashour, A.F. and Platten, A.K. (2006), "Statistical variations in impact resistance of polypropylene fiber-reinforced concrete", *Inter. J. Impact. Eng.*, **32**(11), 1907-1920.
- Banthia, N.P. (1987), "Impact resistance of concrete", PhD Thesis, The University of British Columbia.
- Barr, B. and Baghli, A. (1988), "A repeated drop-weight impact testing apparatus for concrete", *Magazine. Con. Rese.*, **40**(144), 167-176.
- Bull, P.H. and Edgren, F. (2004), "Compressive strength after impact of CFRP-foam core sandwich panels in marine applications", *Comp. Part B*, **35**(6-8), 535-541.
- Erki, M.A. and Meier, U. (1999), "Impact loading of concrete beams externally strengthened with CFRP laminates", *J. Comp. Const.*, **3**(3), 117-124.
- Goldsmith, W. (1960), "Impact: The theory and physical behavior of colliding solids", London Edward Arnold Limited, 145-240.
- Kantar, E. (2009), "Experimental investigation of impact behavior of reinforced concrete beam strengthened with CFRP", Gazi University, Civil Engineering Department, Ph. D. Thesis, 241 page, (In Turkish).
- Kantar, E., Arslan, A. and Anıl, Ö. (2011a), "Effect of concrete compression strength variation on impact behavior of concrete", *J. Faculty of Eng. Architecture of Gazi University*, **26**(1), 115-123.
- Kantar, E., Erdem, T. and Anıl, Ö. (2011b), "Nonlinear finite element analysis of impact behavior of concrete

- beam”, *Mathematical. Comp. Appli.*, **16**(1), 183-193.
- Kishi, N., Konno, H., Ikeda, K. and Matsuoka, K.G. (2002), “Prototype impact tests on ultimate impact resistance of PC rock sheds”, *Int. J. Impact. Eng.*, **27**(9), 969-985.
- Krauthammer, T. (1998), “Blast mitigation technologies: Developments and numerical considerations for behavior assessment and design. structures under shock and impact”, V. Computational Mechanics Publications, 1-12.
- Marar K., Çelik T. and Eren Ö. (2001), “Relationship between impact energy and compression toughness energy of high-strength fiber reinforced concrete”, *Mater. Lett.*, **47**(4-5), 297-304.
- Mindess, S. and Cheng, Y. (1993), “Perforation of plain and fiber reinforced concretes subjected to low-velocity impact loading”, *Cement. Con. Rese.*, **23**(1), 83-92.
- Muszynski, L.C. (1998), “Explosive field test to evaluate composite reinforcement of concrete and masonry walls”, Proceedings of the Second International Conference on Composites in Infrastructure ICCI'98., Tucson Arizona, USA, Edited by H. Saadatmanesh, and M. R. Ehsani, 276-284.
- Murtiadi, S. (1999) “Behavior of high-strength concrete plates under impact loading”, Master Thesis, Faculty of Engineering and Applied Science Memorial University of Newfoundland.
- Nataraja, M.C., Nagaraj, T.S. and Basavaraja, S.B. (2005), “Reproportioning of steel fiber reinforced concrete mixes and their impact resistance”, *Cement. Con. Rese.*, **35**(12), 2350-2359.
- Nagaraj, T.S., Shashiprakash, S.G. and Raghuprasad, B.K., (1993), “Reproportioning concrete mixes”, *ACI Mater. J.*, **90**(1), 50-58.
- Ong, K.C.G., Basheerkhan, M. and Paramasivam, P. (1999), “Resistance of fiber concrete slabs to low velocity projectile impact”, *Cem. Con. Comp.*, **21**(5-6), 391-401.
- Selvi, M. (2008), “Effect of concrete strength variation on the impact behavior”, Gazi University, Civil Engineering Department, Master of Science Thesis, 103 page (In Turkish).
- Siewert, T.A., Manahan, M.P., McCowan, M.P., Holt, J.M., Marsh, F.J. and Ruth, E.A. (1999), “The history and importance of impact testing”, ASTM.
- Tang, T. (2002), “Behavior of concrete beams retrofitted with composite laminates under impact loading”, PhD Thesis, University of Arizona.
- Valipour, H.R., Huynh, L. and Foster, S.J., (2009), “Analysis of RC beams subjected to shock loading using a modified fibre element formulation”, *Comp. Conc., An International J.*, **6**(5).

CC

Nomenclature

- $\Delta E_0(t)$: Energy loss of the hammer at “t” moment
- $u_0(t)$: Mid point deflection on to beam at “t” moment
- $\dot{u}(x, t)$: Velocity from “x” distance at “t” moment
- $T(t)$: Kinetic energy at “t” moment
- $U(t)$: Beam flexure moment energy at “t” moment
- ρ : Specific gravity of concrete
- l : Support span
- B : Beam width
- D : Beam height